UNIVERSITY OF PLYMOUTH

PEARL

Hypertension alters the function and expression profile of the peptide cotransporters PEPT1 and PEPT2 in the rodent renal proximal tubule

Alghamdi, Othman A.; King, Nicola; Andronicos, Nicholas M.; Jones, Graham L.; Chami, Belal; Witting, Paul K.; Moens, Pierre D.J.

Published in:
Amino Acids

DOI:
10.1007/s00726-022-03154-4

Publication date:
2022

Link:
Link to publication in PEARL

Citation for published version (APA):
Alghamdi, O. A., King, N., Andronicos, N. M., Jones, G. L., Chami, B., Witting, P. K., & Moens, P. D. J. (2022). Hypertension alters the function and expression profile of the peptide cotransporters PEPT1 and PEPT2 in the rodent renal proximal tubule. *Amino Acids*, *54*(7), 1001-1011. https://doi.org/10.1007/s00726-022-03154-4

All content in PEARL is protected by copyright law. Author manuscripts are made available in accordance with publisher policies. Wherever possible please cite the published version using the details provided on the item record or document. In the absence of an open licence (e.g. Creative Commons), permissions for further reuse of content
should be sought from the publisher or author.

Download date: 18. Feb. 2025

Hypertension alters the function and expression profile of the peptide cotransporters PEPT1 and PEPT2 in the rodent renal proximal tubule

Othman A. ALGHAMDI [a,] Nicola KING [c], Nicholas M. ANDRONICOS [b], Graham L. JONES [b], Belal CHAMI [e], Paul K. WITTING [d], Pierre D.J. MOENS[b]

[a]Department of Biological Sciences, Faculty of Science, University of Jeddah, KSA

[b]School of Science and Technology, University of New England, Armidale, NSW 2351, Australia

[c]School of Biomedical Sciences, Faculty of Health, University of Plymouth, Plymouth PL4 8AA, UK

[d]Discipline of Pathology, Sydney Medical School, Charles Perkins Centre, The University of Sydney, NSW 2006, Australia

[e]Sydney Dental School, The Faculty of Health and Medicine, The University of Sydney, NSW 2006, Australia

Correspondence to: Nicola King

School of Biomedical Sciences, University of Plymouth, Plymouth. PL4 8AA.

Email: Nicola.king@plymouth.ac.uk

Tel.: +441752 584969

Fax: +441752 586788

Acknowledgements:

This work was supported by the Saudi Ministry of Higher Education, University of New England, and University of Jeddah. We would also like to thank Mr. Brian Cross and Mr. Jonathon Clay for their excellent technical assistance.

Abstract

Hypertension is a major risk factor for kidney and cardiovascular disease. The treatment of hypertensive individuals by selected ACE inhibitors and certain di-and tripeptides halts the progression of renal deterioration and extends life-span. Renal reabsorption of these low molecular weight substrates are mediated by the PEPT1 and PEPT2 cotransporters. This study aims to investigate whether hypertension and ageing affects renal PEPT cotransporters at gene, protein expression and distribution as well as function in the superficial cortex and the outer medulla of the kidney. Membrane vesicles from the brush border (BBMV) and outer medulla (OMMV) were isolated from the kidneys of young Wistar Kyoto (Y-WKY), young spontaneously hypertensive (Y-SHR), and middle aged SHR (M-SHR) rats. Transport activity was measured using the substrate, β-Ala-Lys (AMCA). Gene expression levels of PEPT genes were assessed with qRT-PCR while renal localisation of PEPT cotransporters was examined by immunohistochemistry with Western Blot validation. The K_m and V_{max} of renal PEPT1 were decreased significantly in SHR compared to WKY BBMV, whilst the V_{max} of PEPT2 showed differences between SHR and WKY. By contrast to the reported cortical distribution of PEPT1, PEPT1-staining was detected in the outer medulla, whilst PEPT2 was expressed primarily in the cortex of all SHR; PEPT1 was significantly upregulated in the cortex of Y-SHR. These outcomes are indicative of a redistribution of PEPT1 and PEPT2 in the kidney proximal tubule under hypertensive conditions that has potential repercussions for nutrient handling and the therapeutic use of ACE inhibitors in hypertensive individuals.

Key Words: Hypertension, PEPT1 and PEPT2, Ageing, Di-and tripeptides.

Introduction

Hypertension is considered a leading cause of kidney damage second only to diabetes in the USA (Health United States, 2011). Uncontrolled chronic hypertension increases the incidence of chronic renal failure and cardiovascular disease (CVD) (National High Blood Pressure Education Program Coordinating Committee, 1997; Sarnak et al., 2003). Long-lasting hypertension can also result in functional and structural changes in the kidney and cardiovascular system, which are associated with an increase in mortality and morbidity.

The development of kidney damage in spontaneously hypertensive rats (SHR) resembles the pathogenesis of human nephropathy observed in essential hypertension (Feld et al., 1990). It has been shown that three weeks treatment with the angiotensin converting enzyme (ACE) inhibitor, quinapril delayed histopathological modifications in the kidneys of 19 months old SHR rats (Komatsu et al., 1995). Various other ACE inhibitors have also been shown to exert renoprotective and life prolonging activities in the stroke prone SHR (Feld et al., 1990; Linz et al., 1998; Lee et al., 1995). In humans, the available clinical data indicates that controlling high blood pressure with the ACE inhibitor, ramipril for three years protected the kidneys from functional deterioration in patients with hypertension and chronic non-diabetic nephropathy (Nephropathy-REIN Study, 1997). Although the precise role for PEPT cotransporters in ACE inhibitor uptake in the kidney is currently debated, it is known that commonly used moieties such as quinapril (Akarawut et al., 1998), ramipril (Knütter et al., 2008), and perindopril (Lin et al., 1999) are substrates for these renal PEPT cotransporters.

The mammalian proton-coupled oligopeptide transporters PEPT1 and PEPT2 are capable of recapturing all enzymatically hydrolysed or filtered di-and-tripeptides in the proximal tubule of the kidney and play an important role in balancing protein intake in accordance with physiological necessities (Smith et al., 2013). PEPT1 and PEPT2 are also responsible for the reabsorption of a broad-range of pharmacologically important agents

including some β-lactam antibiotics, antiviral prodrugs, anti-tumour drugs, and selected ACE inhibitors (Smith et al., 2013; Brandsch et al., 2008). In the original publications describing the isolation and cloning of PEPT1 and PEPT2 from the rat, RNA corresponding to each transporter were detected by RT-PCR and Northern blotting respectively in the kidney (Saito et al, 1995; Saito et al., 1996). A more precise localisation followed with PEPT1 identified in the superficial cortex, renal brush border membrane vesicles (BBMV) and S1 (or early cortex) segments of the proximal tubule (Shen et al., 1999; Smith et al., 1998). By contrast, PEPT2 was identified in the deep cortex/outer medulla and segments S2 and S3 (late/outer stripe of the outer medulla) (Shen et al., 1999; Smith et al., 1998). We have previously shown that ageing leads to a change in the expression profiles of these transporters in the rat kidney where PEPT1 in older rats was detected in outer medullary membrane vesicles (OMMV) and PEPT2 in BBMV (Alghamdi et al., 2019). Given this potential for a change in distribution of the PEPT transporters it was considered important to investigate how other conditions may affect PEPT transporter expression and activity in the kidneys. Therefore, the aim of this study was to comprehensively investigate, for the first time, the effects of hypertension on PEPT1 and PEPT2 in the rat kidney at the gene and protein level, including expression and activity.

Material and Methods

Materials

β-Ala-Lys (AMCA) was obtained from Bio Trend Chemicals (Cat. No: BP0352, Destin, USA). Antibodies for PEPT1, PEPT2, and β-Actin were from SANTA CRUZ (Cat No: sc-373742, sc-19918, and sc-47778 respectively, Dallas, USA). TSA-Cy 3.5 amplification kit was from PerkinElmer. Sudan Black B was from Sigma. Primers were purchased from GeneWorks and Sigma. ISOLATE II RNA Mini Kit (Cat No: Bio-52072), Tetro cDNA Synthesis Kit (BIO-

650430), and SensiFAST™ SYBR (Cat No:BIO 98005) were from BIOLINE (Sydney Australia). All other chemicals and consumables used in this study were of analytical grade.

Animal Models

Young adult and middle-aged spontaneously hypertensive (Y-SHR and M-SHR) and young adult Wistar-Kyoto (Y-WKY) rat groups were purchased from the Animal Resources Centre (ARC) Australia (originally from Charles River) at two age groupings: (1) Y-WKY (5-6 months), (2) Y-SHR (5-6 months), and (3) M-SHR (12 months). As recommended by the ARC, the mean arterial pressure (MAP) was monitored for all rats in each of the assigned groups with a pulse transducer-cuff attached to the tail. The transducer was connected to an NIBP controller, which employed "Labchart" software to monitor the mean arterial pressure in real time (baseline MAP: 134.1 ± 1.7 for Y-WKY, 185.2 ± 4.8 for Y-SHR, and 228.2 ± 4.4mmHg for M-SHR). When required, animals were sacrificed by stunning and cervical dislocation, and their kidneys were snap frozen in liquid nitrogen prior to placing them at -80°C for later analyses.

Isolation and quality assessment procedures for BBMV and OMMV

Brush border membrane vesicles were prepared from superficial slices of the kidney cortex (BBMV) and thin slices of the outer medulla (OMMV) as described elsewhere (Alghamdi et al., 2017a; Alghamdi et al., 2017b). Measurements of the enzyme activity and enrichment of leucine aminopeptidase (LA) and alkaline phosphatase (AP) were used as biomarkers to evaluate the quality of the isolated BBMV and OMMV. Vesicles were deemed suitable for subsequent assays providing they were enriched >10 fold in LA and AP compared to the crude supernatant. Bradford's method was used for protein quantification as described previously (Alghamdi et al., 2017a; Alghamdi et al., 2017b).

Uptake of β-Ala-Lys (AMCA) by BBMV and OMMV

The uptake of the fluorophore-conjugated dipeptide β-Ala-Lys (AMCA) by BBMV and OMMV isolated from WKY and SHR rat groups was measured as described previously (Alghamdi et al., 2017b). This entailed using the fluorophore-conjugated dipeptide, β-Ala-Lys (AMCA), which was prepared to its maximum soluble concentration 1 mg/ml (2.32 mM, according to Bio Trend) in extravesicular buffer containing (in mM): 100 KH_2PO_4, 100 mannitol, and 10 2-(N-Morpholino) ethanesulfonic acid (MES)-Tris (pH 6.6). The experiment was started by mixing vesicles (containing 120 or 45 µg proteins) with an appropriate volume of the incubating buffer and with different concentrations of β-Ala-Lys (AMCA) (5–2000 µM) to a total volume of 250 µl in Eppendorf tubes. These tubes were wrapped with aluminium foil and left at 20 °C for 20 min. After that, the transport was stopped by adding the mixture into centrifuge tubes containing 5 ml of ice-cold extravesicular buffer prior to spinning at 31,000 ×g for 20 min at 4 °C. The supernatant was discarded, and the pellet was washed in the centrifuge tubes 3 times, each with 3 ml of the ice-cold extravesicular buffer. This was followed by re-suspending the pellet in 500 µl of the extravesicular buffer using 21 ×1/5 gauge needle attached to a 1 ml syringe. Suspensions were transferred into 96-well black microplates in triplicate by pipetting 165 µl in each well. Furthermore, 500 µl from each wash 1–4 was also checked to confirm the elimination of nonspecific residual substrates. A microplate fluorimeter was used to measure fluorescence emission from 400 to 700 nm with 5 nm steps at an excitation wavelength of 350 nm, and the maximal emission reading at 455 nm. The experiments were repeated at least 4 times using different vesicles isolated from kidneys isolated from different rats and age groupings.

Immunofluorescence imaging

Fluorescence imaging of PEPT1 and PEPT2 cotransporters in the kidneys of Y-WKY, YSHR, and M-SHR rat groups was carried out as described previously (Alghamdi et al., 2018). Snap-frozen kidney samples embedded in Optimal Cutting Temperature Compound (OCT) were cut into 7 micron sections using a cryostat (Leica CM 1850) maintained at − 18 °C. Three sections from 3 different groups (Y-SHR, M-SHR and Y-WKY) were mounted onto Superfrost Plus slide (Thermo Scientific) and air-dried for 30 min at 22 °C. A control was prepared for each specimen on a separate Superfrost Plus slide. The slides were then wrapped with aluminium foil prior to transferring to a − 80 °C freezer for later use. In this way, the tissue architecture was partially protected from moisture damage when taking them out again for staining. To account for the high autofluorescence produced by kidney tissues, slides were blocked with 0.3% (w/v) Sudan Black B (SBB). In addition, Tyramide Signal Amplification (TSA) Systems (PerkinElmer) was used in this experiment as the affinity of the fluorescently labelled antibodies was affected. By this method, it was also possible to probe the tissues with the same antibodies used in Western blotting. Where required, the foil-wrapped slides were taken out of the freezer and equilibrated at 22 °C for 30 min prior to fixing in ice-cold acetone for 20 min. After that, they were gently washed with water and incubated with 0.3% v/v H_2O_2 for 15 min to quench endogenous peroxidase activity. The slides were washed three times with TBS-T buffer containing the following in mM: 150 NaCl, 20 Tris–HCl

(pH 7.5) and 0.1% Tween 20, followed by 1 h incubation with either 1:400 (v/v) mouse monoclonal anti-PEPT1 or goat polyclonal anti-PEPT2 for 1 h at RT. This was followed

by three times washing with TBS-T and incubation with secondary antibodies goat/antimouse or mouse/antigoat accordingly in 1:300 (v/v) dilution. After removing the secondary antibodies by washing three times with TBS-T, 1:50 (v/v) TSA-CY 3.5 was added to the slides for 10 min, followed by washing three times with TBS-T prior to applying SBB (0.3%

w/v in 70% v/v ethanol/H_2O) for 30 min. Finally, the sections were washed with TBS-T for 10 min and then mounted with Dako cytomation fluorescent mounting medium containing DAPI (Dako, USA) and placed under a coverslip. Control slides containing the same sections were used to confirm the suppression of AF in SBB-treated sections, and to examine the specificity of the staining by probing the sections with only secondary antibodies (no primary antibody). A TI eclipse (Nikon corporation, Tokyo, Japan) equipped with a colour-cooled DXM1200C digital camera was used for fluorescence imaging. The optimum conditions of gain and exposure time were established in a preliminary experiment based on the AF level of untreated and SBB-treated sections of all age groups. Exposure time was set to 300 ms and the gain was set to 6.3. Images of resolution 1280 × 1024 px were acquired for the blue, green, red channels and a brightfield.

Immunoblotting

Western blotting was used to semi-quantify the band intensities of PEPT1, PEPT2 and their corresponding β-actin proteins in all rat groups, as described previously (Alghamdi et al., 2017a). BBMV and OMMV containing 45 µg protein/sample were mixed in Eppendorf tubes with the loading buffer containing 6% sodium dodecyl sulphate (SDS), 0.3% bromophenol blue, 30% glycerol, 5% β-mercaptoethanol and 150 mM Tris–HCl (pH 6.8). They were transferred to a boiling water bath at 100 °C for 5 min. After that, the tube contents were loaded onto Mini-PROTEAN Bio-Rad Gels 4-20% and the first well was always loaded with 5 µl of Precision Plus Protein Standards as a molecular weight control ladder. Gels were run at 120 V constant voltage for 40-90 min. The gels were then blotted with nitrocellulose membrane (semi-dry system) at 120 mA for 3 h. The membranes were stripped for 15 min

as described by Kaur and Bachhawat (2009) and incubated overnight with blocking buffer 5% skim milk dissolved in TBS-T buffer containing (in mM) 150 NaCl, 20 Tris–HCl (pH 7.5) and 0.1% Tween 20. The membranes were then incubated with either mouse monoclonal anti-PEPT1 for 1 h at room temperature (RT) or with goat polyclonal anti-PEPT2 overnight at 4 °C. This was followed by an hour's incubation with HRP-conjugated goat anti-mouse and mouse anti-goat IgG, respectively, at RT. Between probing with the primary and secondary antibodies and after incubation with the secondary antibodies, the membranes were washed three times for 10 min with TBS-T buffer. Protein bands were detected using ECLTM Western Blotting Analysis System (GE Healthcare) according to the manufacturer's instructions. Scanned pictures of Hyperfilm ECL were taken using BIO-RAD GEL DOC EQ system. The membranes were transferred to a stripping buffer containing (in mM) 100 β-mercaptoethanol, 62.5 Tris–HCl (pH6.7) and 2% SDS at 55 °C for 30 min, followed by 2 x 10 min washes with TBS-T. Then they were incubated with the blocking buffer and reprobed with anti-β-actin (mouse monoclonal) antibodies, following the steps described above. BIO-RAD GEL DOC EQ system and Quantity One software were used to quantify the band intensities of PEPT1 and PEPT2, relative to their corresponding β-actin bands on Hyperfilm ECL (GE Healthcare) (Figure 5 & 6).

Real-Time RT-qPCR

Real-time RT-qPCR was used to relatively quantify the expression of PEPT1 and PEPT2 as described previously (Alghamdi et al., 2018). Biopsies of renal tissues (18 mg) were removed

from the superficial cortex and outer medulla of renal tissue for each rat group (samples were taken from kidneys previously

snap-frozen for storage). Total RNA was isolated from these tissues using ISOLATE II RNA Mini Kit (BIOLINE, Cat No: Bio-52072). Three quality control experiments were performed prior to proceeding to cDNA synthesis: (1) the RNA purity and quantity was checked by measuring the absorbance at 260/280 ratio > 1.9 with a NanoDrop UV–Vis spectrophotometer (Thermo Scientific); (2) the RNA integrity was confirmed by 1% w/v agarose gel where the intensity of tRNA 28S was twice that of the 18S bands; (3) possible contamination by genomic DNA was checked by adding 10 ng of RNA from each sample to 0.5 μM forward and reverse PEPT primers, 5 μL SYBR green, and 3 μL nuclease-free water. These experiments, which were run under the same conditions as described below for the

cDNA samples, did not show any amplification indicating good RNA isolation. cDNA synthesis of isolated total RNA samples was performed in 96-well plates (T 100™ Thermal Cycler, Bio-Rad) using Tetro cDNA Synthesis Kit (BIOLINE). Total RNA (5 μg) was mixed with Oligo (dT)18, Random Hexamer, dNTP mix, RiboSafe RNase Inhibitor and Tetro Reverse Transcriptase according to the manufacturer's instructions. The resulting cDNA was then used to perform q-PCR, by mixing 5 μL SensiFAST™ SYBR (Bioline) with cDNA

(10 ng RNA; the use of RNA concentration as the concentration for cDNA is recommended and since the isolated RNA was diluted in RNAse free water, it was possible to blank against this water using a nanodrop spectrophotometer) and 500 nM forward and reverse primers (Table 1) in a 384-well plate (in duplicate). Primers for β-Actin, and SDHA (succinate

dehydrogenase) were used as reference genes. The loaded 384-well plate was read on a QRT-PCR Bio-Rad CFX plate reader. This was started by denaturation at 95 °C for 2 min, followed by amplification for 39 cycles of denaturation, annealing and extension as follows:

95 °C/10 s, 60 °C/20 s, 72 °C/15 s. These reactions were always followed by 1 cycle step to generate the melt curve at 95°C/0.5 s, 65°C/0.5 s, 95°C/5 s. The ΔΔ Cq method of the Bio-Rad CFX Manager 3.1 was used to determine differences between samples by normalising with two reference genes. All samples produced single peaks, indicating specific product amplification. The predicted sizes of products were examined by running samples (5 μL) on 2% agarose gel, which showed the expected sizes. Before these steps, two samples were only converted to cDNA to check the specificity of the primers. The methods used complied with the MIQE guidelines for the minimum information of RT-qPCR experiments (Bustin et al., 2009).

Data Analysis and Statistics

Data in Figure 1 and 2 were fitted using least squares analysis to the Michaelis-Menten curve in Fig P (version 3). The equation $V_{max} = [S] / K_m + [S]$ was then used to calculate K_m and V_{max}. Data in Figs 1-2 and 7-8 are shown as means ± S.E. Immunofluorescence staining (Figs 3-4) and Western Blots (5-6) are representative of a number of repeats as stated in the Figure legends. Data were compared using ANOVA with a post hoc Tukey test. $P<0.05$ was considered significant. Statistical analysis was carried in Instat (version 3.05).

Results

Body and Kidney weights of the different rat groups

Table 2 shows the body and kidney wet weights of all the different rat groups used in this study. The body weight of the Y-WKY was significantly greater compared to Y-SHR, which were significantly lighter than the M-SHR. In contrast, kidney wet weight for the Y-SHR was

significantly greater compared to the same tissue isolated from Y-WKY. Kidneys from M-SHR were significantly heavier than the same tissues obtained from both the Y-WKY and Y-SHR.

Uptake of β-Ala-Lys (AMCA) as a function of concentration

The Michaelis-Menten curves (R^2 >0.9) shown in Figure 1 and Figure 2 are representative of the rate of uptake (ΔF/mg/min) of β-Ala-Lys (AMCA) as a function of concentration (μM) into BBMV and OMMV isolated from the kidneys of Y-WKY, Y-SHR, and M-SHR rats. Kinetic parameters, V_{max} and K_m for all vesicles isolated from all groups were analysed to investigate the effect of hypertension and ageing on the biological activity of the small peptide transporters, PEPT1 and PEPT2 (Table 3). Comparing data for OMMV and BBMV, it is apparent that OMMV from Y-WKY showed significantly higher affinity, but lower capacity than BBMV from the same Y-WKY rats (P=0.01). However, the opposite was observed in the transport capacity by OMMV prepared using kidneys from Y-SHR, which was significantly higher than in BBMV (P=0.01) with no overall changes in affinity. Interestingly, there were no significant changes in the transport affinity and capacity when isolated BBMV and OMMV from M-SHR rat groups were compared (table 3).

A similar comparison of BBMV from Y-SHR kidney showed significantly lower transport capacity (P=0.01), but significantly higher affinity (P=0.03) than BBMV from Y-WKY kidney. In addition, BBMV from M-SHR kidney demonstrated significantly higher transport capacity than BBMV from Y-SHR kidney (P=0.001) and higher affinity ($p<0.05$). Comparing within the OMMV groups, the transport capacity of OMMV was significantly increased with Y-WKY having a lower V_{max} than Y-SHR (P=0.01), and Y-SHR having a lower V_{max} than M-SHR (P=0.001); although, there were no significant changes in affinity (Table 3).

Visualisation of PEPT Cotransporters using Immunofluorescence

It has been previously reported that PEPT1 and PEPT2 cotransporters are sequentially distributed along the proximal tubule in segment 1 and segment 3 respectively (Shen et al., 1998). WKY and SHR rat models were employed in this study to identify whether hypertension and ageing disturbed this normal distribution pattern. As shown in Figure 3, the presence of PEPT1 protein in Y-WKY and hypertensive Y-SHR rat groups was largely restricted to the superficial cortex with a notable decrease in PEPT1-staining in renal tissues from the latter group. However, the M-SHR group revealed a wider distribution of PEPT1 with PEPT1-staining detected in the superficial cortex through to the medullary region of the same kidney.

In addition, PEPT2 protein was present in the outer medulla of all rat groups with lower expression in SHR groups as judged by a lower level of PEPT2-staining. Notably, the PEPT2 protein was absent in the superficial cortex of Y-WKY kidneys, but present in that kidney region in renal tissue from SHR rats (Figure 4).

Immunoblotting

The presence of PEPT1 and PEPT2 cotransporters in the superficial cortex and outer medulla was further quantified in the kidneys of WKY and SHR rat groups using Western blot. Similar to the immunofluorescence experiments, SHR groups showed the presence of PEPT1 labelling in regions where they are anticipated to be absent in the proximal tubule (Figure 6) (Shen et al., 1999). Significant differences in PEPT1 and PEPT2 proteins were determined in all rat groups as judged after measuring the relative intensity of the bands shown in Figure 7, (ANOVA, $P = 0.0004$ and $4x10^{-9}$ respectively). This was followed by post-hoc t-test which revealed a significant decrease in the intensity ratio of PEPT1 protein in renal BBMV from Y-SHR group compared to renal BBMV from Y-WKY group ($P=0.02$). However, the amount of PEPT1 in renal BBMV from M- SHR was significantly higher than in kidneys from both other groups ($P=0.03$ and 0.01 respectively) and was also present in OMMV in similar amount.

Furthermore, the intensity ratios of PEPT2 protein in renal OMMV isolated from Y-WKY was significantly higher than the corresponding renal OMMV isolated from Y-SHR and M-SHR groups (P=0.04, and 0.03 respectively). PEPT2 protein was also present in renal BBMV (where it is anticipated to be absent (Shen et al., 1999)) isolated from SHR groups.

RT-qPCR

The expression of SLC15A1 (PEPT1) and SLC15A2 (PEPT2) genes were quantified in the superficial cortex and outer medulla of the renal proximal tubule, respectively. The relative normalised values extracted from Bio-Rad CFX Manager 3.1 were statistically analysed and plotted as shown in Figure 8. The relative expression of SLC15A1 gene in Y-SHR group was significantly higher (by up to 10-fold) than Y-WKY (P=0.037) and 15 fold higher than that determined for M-SHR (P=0.031). By contrast, SLC15A2 in SHR groups was decreased by approximately 2-fold compared to mRNA expression determined in kidney tissues from the WKY group, although this decrease did not reach significant difference.

Discussion

Outcomes from this study address whether changes in PEPT membrane transporters occur as a result of hypertension and ageing in the superficial cortex and outer medulla regions of the kidney. The first experiments carried out investigated the activity of the transporters in BBMV and OMMV (Figs 1 and 2 and table 3). This demonstrated that there were significant differences between the K_m and V_{max} in the different vesicles from the different rat groups. The remaining experiments investigated the expression of the two transporters in different regions of the kidney (Figure 3, 4 and 8) or in BBMV and OMMV (Figures 5-7) in the Y-SHR, M-SHR and Y-WKY. At the protein level PEPT1 was present in cortex and BBMV of all groups and additionally was present in the outer medulla and OMMV of the Y- and M-SHR (fig 3 and

7). On the other hand PEPT2 was present in the outer medulla and OMMV of all groups and the cortex and BBMV of the Y- and M-SHR (Figures 4 and 7). At the gene level PEPT1 expression in cortex was significantly greater in the Y-SHR compared to the other groups, whilst there were no changes in PEPT2 expression in the outer medulla across all groups. Taken together these results suggest that the PEPT cotransporters are redistributed in chronic uncontrolled hypertension, which could have implications for the renal handling of oligopeptides and peptidomimetic drugs.

PEPT1 and PEPT2 cotransporters are responsible for transporting di- and tripeptides besides peptidomimetic drugs with clinical and pharmacological relevance such as some ACE-inhibitors and β-lactam antibiotics (reviewed in Smith et al., 2013; Rubio-Aliaga & Daniels, 2008). Ageing is associated with a decrease in glomerular filtration rate that may slow the elimination of drugs and hinder nutrient reabsorption (Burris et al., 2016). Certainly, there was an increased capacity for β-Ala-Lys (AMCA) uptake in BBMV from M-SHR and OMMV from Y-SHR and M-SHR (table 3). It is possible to speculate that these observations suggest that the elderly and those with chronic uncontrolled hypertension may require a lower dosage of drugs that are PEPT substrates; however this generalisation would need testing in a human population.

This is the first study to investigate whether Y-SHR and M-SHR rat groups conserve the normal distribution of PEPT1 and PEPT2 in S1 and S3 segments of the renal proximal tubule respectively as reported in this work. We have demonstrated evidence of significant PEPT1 cotransporter expression and functionality in the outer medulla and/or OMMV of M-SHR rat group (Figure 3, 5-7). Similarly, PEPT2 protein was found in the superficial cortex and BBMV of Y-SHR and M-SHR rat groups with significantly higher abundance in M-SHR (Figure 4, 5-7). The presence of PEPT1 and PEPT2 in other regions of the renal proximal tubule (ordinarily absent), has only been reported in rat kidneys following an uninephrectomy

(Tramonti et al., 2006). It should however be noted that the antibodies used here are different to those used by Shen et al (1998).

It is possible to speculate that one possible explanation for this redistribution could be changes in the demand for amino acids for glutathione synthesis. This is supported by independent studies which reported: (1) a decreased level of glutathione accompanied with increased activity and protein levels of glutathione synthetase with ageing (Thiab et al., 2015), and (2) a significant decrease in the reabsorption of Cys-Gly, a break-down product of GSH, in PEPT2-deficient animals (Rubio-Aliaga et al., 2003; Frey et al., 2006; Frey et al., 2007). Although in this study, we used different age groups (because of the shorter lifespan of SHR) these available data may be explained in part through downregulation of PEPT2 in SHR rat groups, but upregulation of PEPT1 in M-SHR.

The poor correlation between gene and protein expression in this study could possibly be due to the inter-regulation processes between transcription, translation, and protein turnover (Tian et al., 2004; Vogel et al., 2010; Schwanhausser et al., 2011). For example, Dalmasso *et al.* (2011) showed that post-transcriptional regulation of SLC15A1 "hPepT1" in differentiating Caco2-BBE cells by microRNA-92b could reduce hPepT1 transport activity as well as protein and gene expression.

Conclusions

In conclusion, our findings suggest that uncontrolled hypertension can affect localisation, expression, and function of the renal-type PEPT1 and PEPT2 cotransporters. This could have important implications for the maintenance and optimisation of nutritional amino acids and peptidomimetic drug dosage in hypertensive individuals. A greater understanding of

hypertension-induced changes in PEPT1 and PEPT2 expression, localisation and functionality within the renal system could lead to improvements in the management of hypertensive patients.

Declarations

Funding: This work was supported by the Saudi Ministry of Higher Education, University of New England, and University of Jeddah.

Conflicts of Interest: None to declare

Availability of data and material: Available on request

Code Availability: NA

Author Contributions: OA performed the research, analysed the data and wrote the first draft of the paper. NK analysed the data and substantially edited the first draft. NA and BC and PW contributed methods to the paper and analysed the results. PM conceived the study and edited the final draft.

Ethics Approval: This study was approved by the Animal Ethics committee of the University of New England, and complied with the *Guide for the care and use of laboratory Animals* published by the US National Institute of Health (NIH Publication No. 85-23, revised 1996).

References

Akarawut, W., Lin, C.J., Smith, D.E., 1998. Noncompetitive inhibition of glycylsarcosine transport by quinapril in rabbit renal brush border membrane vesicles: effect on high-affinity peptide transporter. J Pharmacol Exptl Therapeut. 287, 684-690.

Alghamdi, O.A., King, N., Andronicos, N.M., Jones, G.L., Chami, B., Witting, P.K., Moens P.D.J. 2018. Molecular changes to the rat renal transporters PEPT1 and PEPT2 due to ageing. Mol Cell Biochem. 452, 71-82.

Alghamdi, O.A., King, N., Jones G.L., Moens, P.D.J., 2017a. Kinetic Measurements of Di- and Tripeptide and Peptidomimetic Drug Transport in Different Kidney Regions Using the Fluorescent Membrane Potential-Sensitive Dye, DiS-C3-(3). J Membr Biol. 250, 641-649.

Alghamdi, O.A., King, N., Jones, G.L., Moens, P.D.J., 2017b. A new use of beta-Ala-Lys (AMCA) as a transport reporter for PEPT1 and PEPT2 in renal brush border membrane vesicles from the outer cortex and outer medulla. Biochim Biophys Acta. 1860, 960-964.

Brandsch, M., Knutter, I., Bosse-Doenecke, E., 2008. Pharmaceutical and pharmacological importance of peptide transporters. J pharmacy pharmacol. 60, 543-585.

Burris, J.F., Tortorici, M.A., Mandic, M., Neely, M., Reed, M.D., 2016. Dosage adjustments related to young or old age and organ impairment. J Clinical Pharmacol. 56, 1461-1473.

Bustin, S.A., Benes, V., Garson, J.A., Hellemans, J., Huggett, J., Kubista, M., Mueller, R., Nolan, T., Pfaffl, M.W., Shipley, G.L., Vandesompele, J., Wittwer, C.T., 2009. The MIQE guidelines: minimum information for publication of quantitative real-time PCR experiments. Clin Chem. 55, 611-622.

Dalmasso, G., Nguyen, H.T., Yan, Y., Laroui, H., Charania, M.A., Obertone, T.S., Sitaraman, S.V., Merlin, D., 2011. MicroRNA-92b regulates expression of the oligopeptide transporter PepT1 in intestinal epithelial cells. Am J Physiol. 300, G52-59.

Feld, L.G., Cachero, S., Van Liew, J.B., Zamlauski-Tucker, M., Noble, B., 1990. Enalapril and renal injury in spontaneously hypertensive rats. Hypertension. 16, 544-554.

Frey, I.M., Rubio-Aliaga, I., Klempt, M., Wolf, E., Daniel, H., 2006. Phenotype analysis of mice deficient in the peptide transporter PEPT2 in response to alterations in dietary protein intake. Pflügers Archiv. 452, 300-306.

Frey, I.M., Rubio-Aliaga, I., Siewert, A., Sailer, D., Drobyshev, A., Beckers, J., de Angelis, M.H., Aubert, J., Bar Hen, A., Fiehn, O., Eichinger, H.M., Daniel, H., 2007. Profiling at mRNA, protein, and metabolite levels reveals alterations in renal amino acid handling and glutathione metabolism in kidney tissue of Pept2-/- mice. Physiological Genomics. 28, 301-310.

Health United States, 2011. End-stage renal disease patients, by selected characteristics: United States, selected years 1980–2010. Centers for Disease Control and Prevention The USA.

Knütter, I., Wollesky, C., Kottra, G., Hahn, M.G., Fischer, W., Zebisch, K., Neubert, R.H.H., Daniel, H., Brandsch, M., 2008. Transport of angiotensin-converting enzyme inhibitors by H+/peptide transporters revisited. J Pharmacol Exptl Therapeut. 327, 432-441.

Komatsu, K., Frohlich, E.D., Ono, H., Ono, Y., Numabe, A., Willis, G.W., 1995. Glomerular dynamics and morphology of aged spontaneously hypertensive rats. Effects of angiotensin-converting enzyme inhibition. Hypertension. 25, 207-213.

Lee, R.M., Delaney, K.H., Lu, M., 1995. Perindopril treatment prolonged the lifespan of spontaneously hypertensive rats. J Hypertens. 13, 471.

Lin. C-J., Akarawut, W., Smith, D.E., 1999. Competitive inhibition of glycylsarcosine transport by enalapril in rabbit renal brush border membrane vesicles: interaction of ACE inhibitors with high affinity H+/peptide symporter. Pharmaceut Res. 16, 609-615.

Linz, W., Becker, R.H., Schölkens, B.A., Wiemer, G., Keil, M., Langer, K.H., 1998. Nephroprotection by longterm ACE inhibition with ramipril in spontaneously hypertensive stroke prone rats. Kid int. 54, 2037-2044.

National High Blood Pressure Education Program Coordinating Committee., 1997. The sixth report of the joint national committee on prevention, detection, evaluation, and treatment of high blood pressure. Arch Internal Med. 157, 2413-2446.

Nephropathy-REIN Study., 1997. Randomised placebo-controlled trial of effect of ramipril on decline in glomerular filtration rate and risk of terminal renal failure in proteinuric, non-diabetic nephropathy. The GISEN Group (Gruppo Italiano di Studi Epidemiologici in Nefrologia). Lancet. 349, 1857-1863.

Rubio-Aliaga, I., Daniel, H., 2008. Peptide transporters and their roles in physiological processes and drug disposition. Xenobiotica; the fate of foreign compounds in biological systems. Xenobiotica. 38, 1022-1042.

Rubio-Aliaga, I., Frey, I., Boll, M., Groneberg, D.A., Eichinger, H.M., Balling, R., Daniel, H., 2003. Targeted disruption of the peptide transporter Pept2 gene in mice defines its physiological role in the kidney. Mol Cell Biol. 23, 3247-3252.

Saito H., Okuda M., Terada T., Sasaki S., Inui K., 1995. Cloning and characterization of a rat H+/peptide cotransporter mediating absorption of beta-lactam antibiotics in the intestine and kidney. J Pharmacol Therapeut. 275, 1631-1637.

Saito H., Terada T., Okuda M., Sasaki S., Inui K., 1996. Molecular cloning and tissue distribution of rat peptide transporter PEPT2. Biochim Biophys Acta. 1280, 173-177.

Sarnak, M.J., Levey, A.S., Schoolwerth, A.C., Coresh, J., Culleton, B., Hamm, L.L., McCullough, P.A., Kasicke, B.L., Kelepouris, E., Klag, M.J., Parfrey, P., Pfeffer, M., Raij, L., Spinosa, D.J., Wilson, P.A., 2003. Kidney disease as a risk factor for development of cardiovascular disease: a statement from the American Heart Association Councils on Kidney in Cardiovascular Disease, High Blood Pressure Research, Clinical Cardiology, and Epidemiology and Prevention. Circ. 108, 2154-2169.

Schwanhausser, B., Busse, D., Li, N., Dittmar, G., Schuchhardt, J., Wolf, J., Chen, W., Selbach, M., 2011. Global quantification of mammalian gene expression control. Nature. 473, 337-342.

Shen, H., Smith, D.E., Yang, T., Huang, Y.G., Schnermann, J.B., Brosius, III F.C., 1999. Localization of PEPT1 and PEPT2 proton-coupled oligopeptide transporter mRNA and protein in rat kidney. Am J Physiol. 276, F658-F665.

Smith, D.E., Clemencon, B., Hediger, M.A., 2013. Proton-coupled oligopeptide transporter family SLC15: physiological, pharmacological and pathological implications. Mol Aspects Med. 34, 323-336.

Smith. D.E., Pavlova, A., Berger, U.V., Hediger, M.A., Yang, T., Huang, Y.G., Schnermann, J.B., 1998. Tubular localization and tissue distribution of peptide transporters in rat kidney. Pharmaceut Res. 15, 1244-1249.

Thiab, N.R., King, N., Jones, G.L., 2015. Effect of ageing and oxidative stress on antioxidant enzyme activity in different regions of the rat kidney. Mol Cell Biochem. 408, 253-260.

Tian, Q., Stepaniants, S.B., Mao, M., Weng, L., Feetham, M.C., Doyle, M.J., Yi, E.C., Dai, H.Y., Thorrson, V., Eng, J., Goodlett, D., Berger, J.P., Gunter, B., Linseley, P.S., Stoughton, R.B., Aebersold, R., Collins, S.J., Hanlon, W.A., Hood, L.E., 2004. Integrated genomic and proteomic analyses of gene expression in Mammalian cells. Mol Cellular proteomics. 3, 960-969.

Tramonti. G., Xie, P., Wallner, E.I., Danesh, F.R., Kanwar, Y.S., 2006. Expression and functional characteristics of tubular transporters: P-glycoprotein, PEPT1, and PEPT2 in renal mass reduction and diabetes. Am J Physiol. 291, F972-980.

Vogel, C., Abreu Rde, S., Ko, D., Le, S.Y., Shapiro, B.A., Burns, S.C., Sandhu, D., Boutz, D.R., Marcootte, E.M., Penalva, L.O., 2010. Sequence signatures and mRNA concentration can explain two-thirds of protein abundance variation in a human cell line. Mol Systems Biol. 6, 400.

Figure and Table Legends

Fig 1 The rate of change in fluorescence as a function of β-Ala-Lys (AMCA) concentration incubated with 45 μg protein of BBMV isolated from the kidneys of Y-WKY (dotted line, sqaures), Y-SHR (dashed line, circles), and M-SHR (solid line, triangles) at pH 6.6. The curves were fitted using the Michaelis-Menten equation (R_2 >0.9). Data shown are means ± SE, where n= 6.

Fig 2 The rate of change in fluorescence as a function of β-Ala-Lys (AMCA) concentration incubated with 45 μg protein of OMMV isolated from the kidneys of Y-WKY (dotted line, squares), Y-SHR (dashed line, circles), and M-SHR (solid line, triangles) at pH 6.6. The curves were fitted using the Michaelis-Menten equation (R_2 >0.9). Data shown are means ± SE, where n= 6.

Fig 3 Fluorescent images of kidney cross sections showing immunolocalisation of PEPT1 in the cortex of Y-WKY (A), Y-SHR (B) and M-SHR (C) kidneys by the red immunofluorescent staining TSA-CY 3.5 amplification kit and anti- PEPT1 mouse monoclonal antibody. PEPT1 was also present in the outer medulla and medulla of M-SHR (C and I) and with low presence in Y-SHR (H), but not in Y-WKY kidneys (G). DAPI staining DNA (blue) was merged with

the specifc-PEPT1 staining. Brightfield images were also acquired for the same sections (D-F and J-L). Data shown are taken from a single experiment representative of 4 such experiments.

Fig 4 Fluorescent images of kidney cross sections showing immunolocalisation of PEPT2 in the outer medulla of Y-WKY (A), Y-SHR (B) and M-SHR (C) kidneys by the red immunofluorescent staining TSA-CY 3.5 amplification kit and anti- PEPT2 goat polyclonal antibody. PEPT2 transporter was also present in the cortex of Y-SHR (B) and M-SHR (C), but not in Y-WKY (G) kidneys. DAPI staining DNA (blue) was merged with the specifc-PEPT2 staining. Brightfield images were also acquired for the same sections (D-F and H). Data shown are taken from a single experiment representative of 4 such experiments

Fig 5 Western blotting bands for PEPT1 and PEPT2 proteins with their corresponding β- actin protein bands. (A) Shows the bands of PEPT1 proteins in BBMV isolated from the kidneys of Y-WKY, Y-SHR, and M-SHR rats. (B) Shows the bands of PEPT2 proteins in OMMV isolated from the same groups. Data shown are taken from a single experiment representative of 4 such experiments.

Fig 6 Western blotting bands for PEPT1 and PEPT2 proteins with their corresponding β-actin protein bands. (A) The presence of PEPT1 proteins in OMMV isolated from the kidneys of Y-WKY, Y-SHR, and M-SHR. (B) The presence of PEPT2 protein in BBMV isolated from the kidneys of the same groups. Data shown are taken from a single experiment representative of 4 such experiments.

Fig 7 Bar graphs comparing the relative level of PEPT1 (A) and PEPT2 (B) protein expression in BBMV and OMMV isolated from Y-WKY, Y-SHR and M-SHR. Results are expressed as

the intensity ratio (%) with respect to β-actin. A) * p=0.02 vs. Y-WKY; ** p<0.05 vs. Y-WKY and Y-SHR. B) p<0.05 vs. Y-SHR and M-SHR. Data shown are means ± SE, where n=4-6.

Fig 8 Relative normalised expression of PEPT1 and PEPT2 genes (against two housekeeping genes SDHA, and β-Actin) was measured by QRT-PCR and ΔΔ Cq method using Bio-Rad CFX manager 3.1. These genes are measured in the Cortex (Cox) and Outer medulla (OM) of young adult WKY, young adult SHR, and middle-aged SHR rat kidneys, as colours shown in the graph. * p<0.05 vs Y-WKY and M-SHR. Data shown are means ± SE, where n=5.

Table 1 Primer sequences used for the different genes investigated in this study.

Table 2 Body and kidney weights of the different rat groups used in this study. * p < 0.05 vs young-WKY, ** p < 0.05 vs young-SHR. Data are means ± SE of n=16 kidneys, which were isolated from n=8 rats

Table 3 Comparison of the kinetic parameters, Km (μM) and Vmax (μM/min/mg) for the uptake of β-Ala-Lys (AMCA) in BBMV and OMMV isolated from the Kidneys of WKY and SHR groups. * p < 0.05 vs young OMMV, ** p < 0.05 vs young-WKY BBMV or OMMV, † p < 0.05 vs young-SHR BBMV or OMMV. Data shown are means ± SE of n=6.

Table 1

Gene name	NCBI Ref-Seq	Sense primer 5'-3' (Tm °C)	Antisense primer 5'-3' (Tm °C)	PCR product size (position on Template)
SLC15A1 (PEPT1)	NM-057121.1	GACCAGATGCAGACGGTGAA (54)	AATGAGCGGATACACCACGG (56)	78 bp (1018-1095)
SLC15A2 (PEPT2)	NM-031672.2	TTCTCAGGCACCATCTAGCA (55)	CGGAGAAGATCAGGCAGACC (56)	170 bp (2074-2243)
β-Actb	NM-0311144.3	CGCGAGTACAACCTTCTTGC (59)	CGTCATCCATGGCGAACTGG (60)	70 bp (19-88)
SDHA	NM-130428.1	GCAGGACTGAAGATGGGAGG (56)	ACCGCAGAGATCGTCCATAC (54)	150 bp (499-648)

Table 2

Rat Group	Body Weight (g)	Kidney Weight (g)
Young-WKY	365.6 ± 5.2	1.19 ± 0.019
Young-SHR	340.8 ± 3.1 *	1.28 ± 0.02 *
Middle-aged-SHR	368.5 ± 9.9 **	1.4 ± 0.17 *, **

Table 3

	BBMV (PEPT1)		OMMV (PEPT2)	
Rat Group	V_{max} (ΔF/min/mg)	K_m (μM)	V_{max} (ΔF/min/mg)	K_m (μM)
Y-WKY	1079.9 ± 65.7 *	208.2 ± 48.6 *	713.4 ± 45.3	34.3 ± 11.2
Y-SHR	766.4 ± 38.8 *, **	62.3 ± 14.6 **	1008.1 ± 54.2 **	46.9 ± 12.3
M-SHR	1321.2 ± 70 †	76.1 ± 18.2 **	1239.1 ± 70 **, †	63.5 ± 16.9

Figure 1

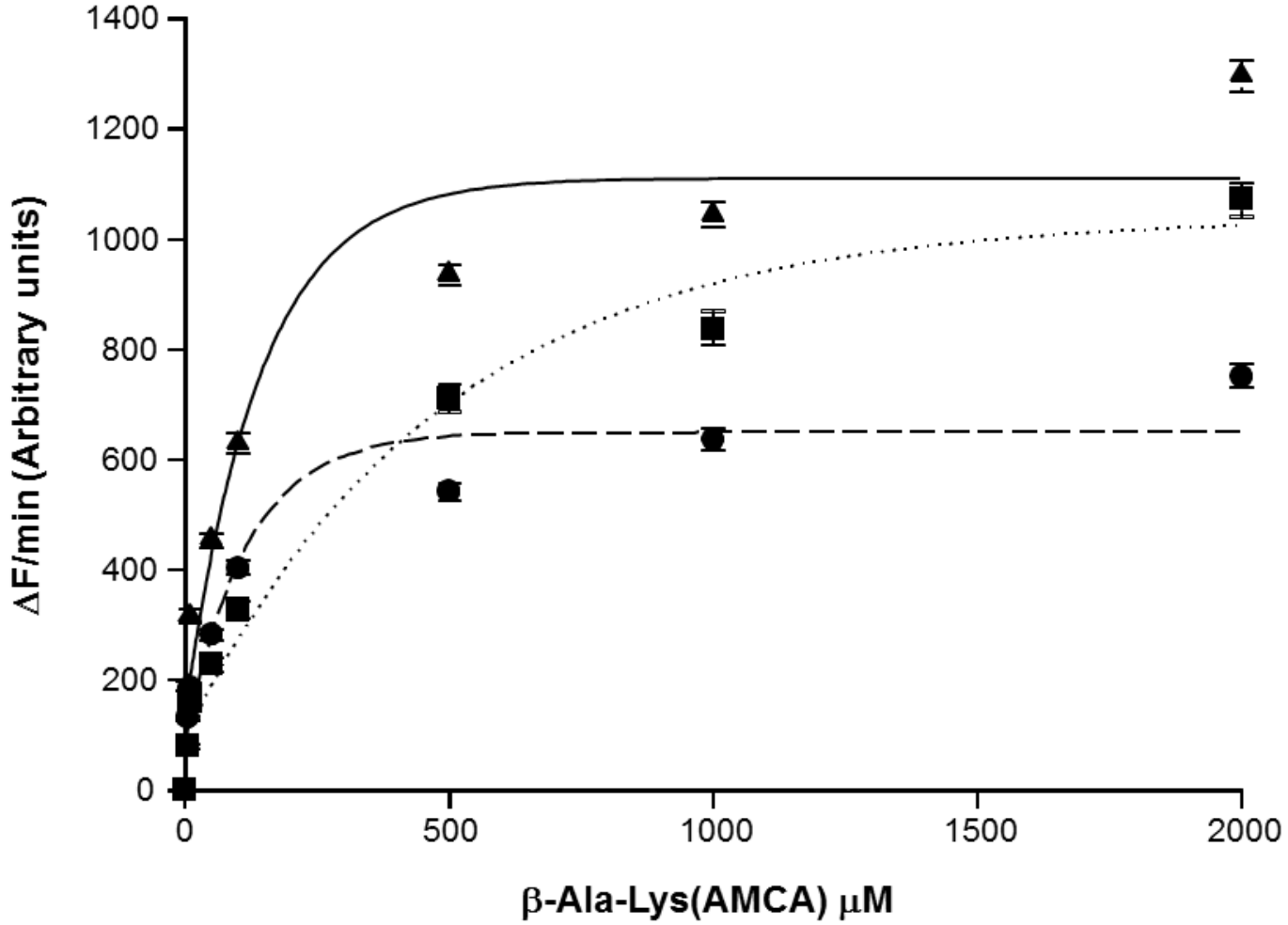
1400
1200
1000
800
600
400
200
0
ΔF/min (Arbitrary units)
0
500
1000
1500
2000
β-Ala-Lys(AMCA) μM

Figure 2

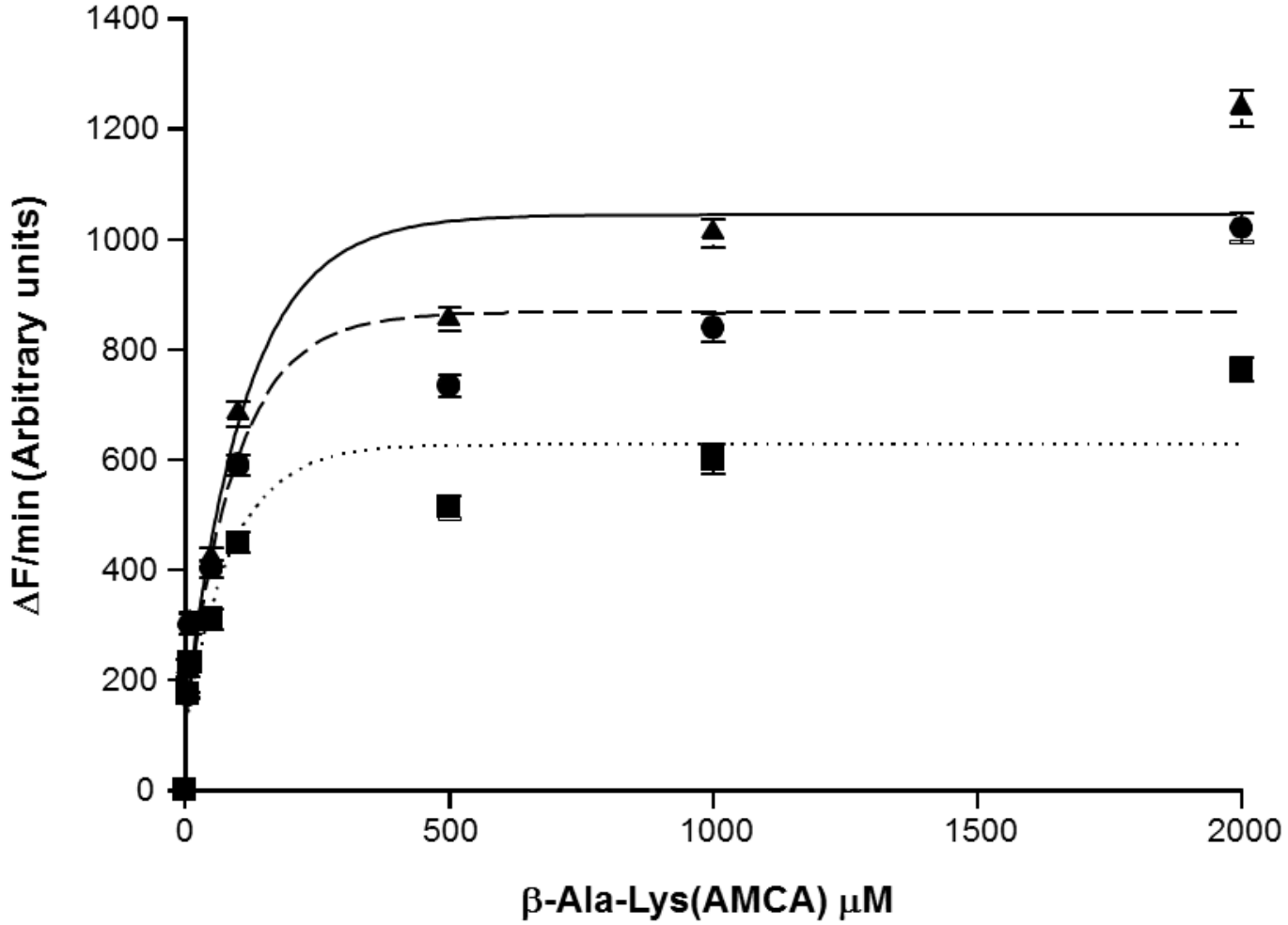
1400
1200
1000
800
600
400
200
0
ΔF/min (Arbitrary units)
0
500
1000
1500
2000
β-Ala-Lys(AMCA) μM

Figure 3

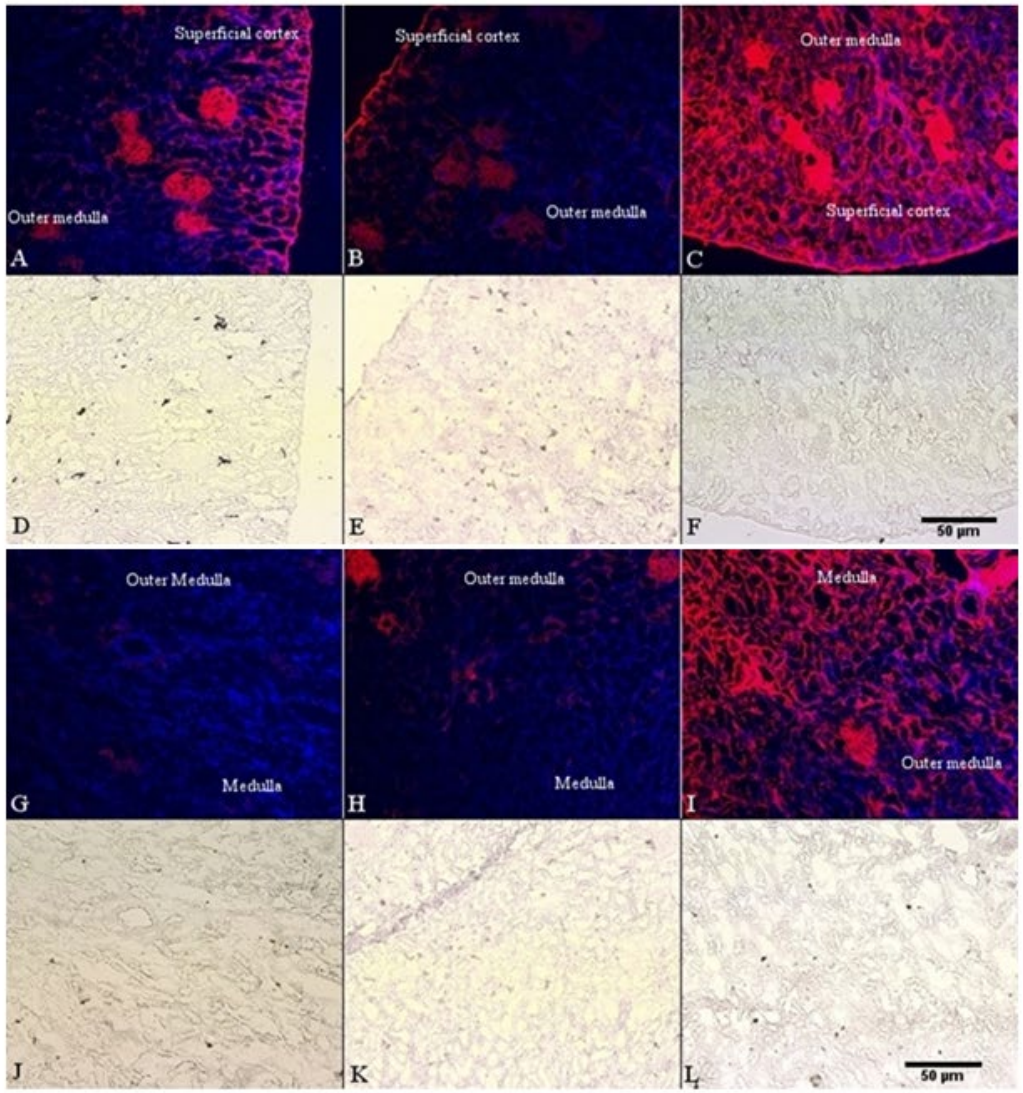
Superficial cortex
Outer medulla
A
Superficial cortex
Outer medulla
B
Outer medulla
Superficial cortex
C
D
E
F
50 µm
Outer Medulla
Medulla
G
Outer medulla
Medulla
H
Medulla
Outer medulla
I
J
K
L
50 µm

Figure 4

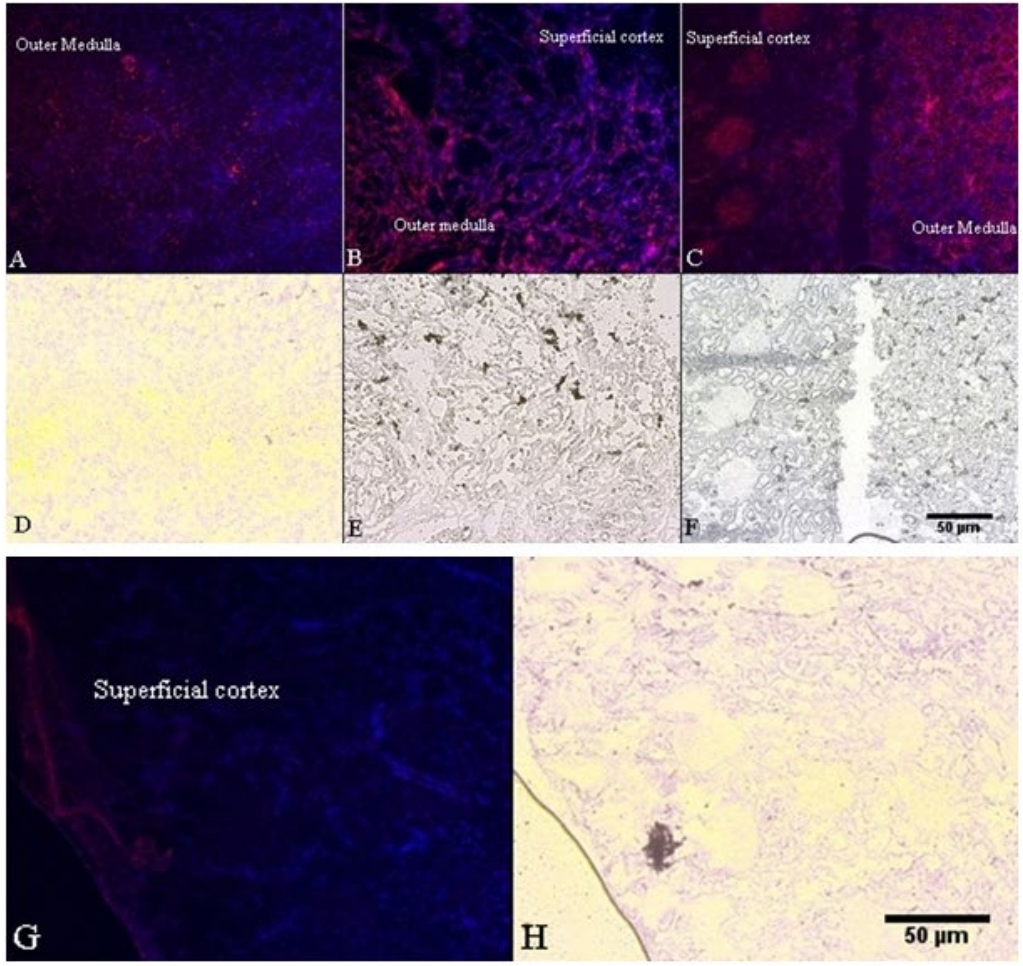
Outer Medulla
A
Superficial cortex
Outer medulla
B
Superficial cortex
Outer Medulla
C
D
E
F
50 µm
Superficial cortex
G
H
50 µm

Figure 5

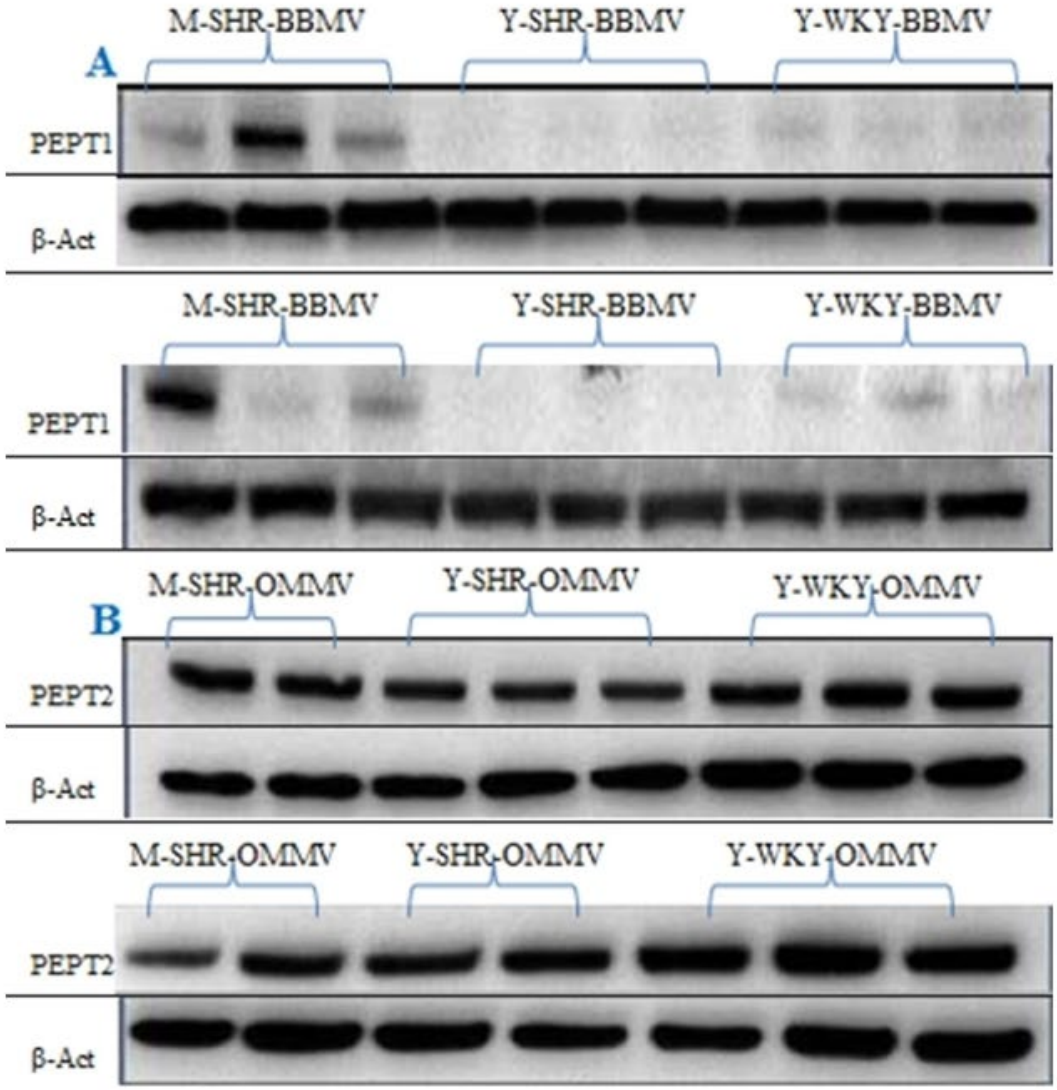
A
M-SHR-BBMV
Y-SHR-BBMV
Y-WKY-BBMV
PEPT1
β-Act
M-SHR-BBMV
Y-SHR-BBMV
Y-WKY-BBMV
PEPT1
β-Act
B
M-SHR-OMMV
Y-SHR-OMMV
Y-WKY-OMMV
PEPT2
β-Act
M-SHR-OMMV
Y-SHR-OMMV
Y-WKY-OMMV
PEPT2
β-Act

Figure 6

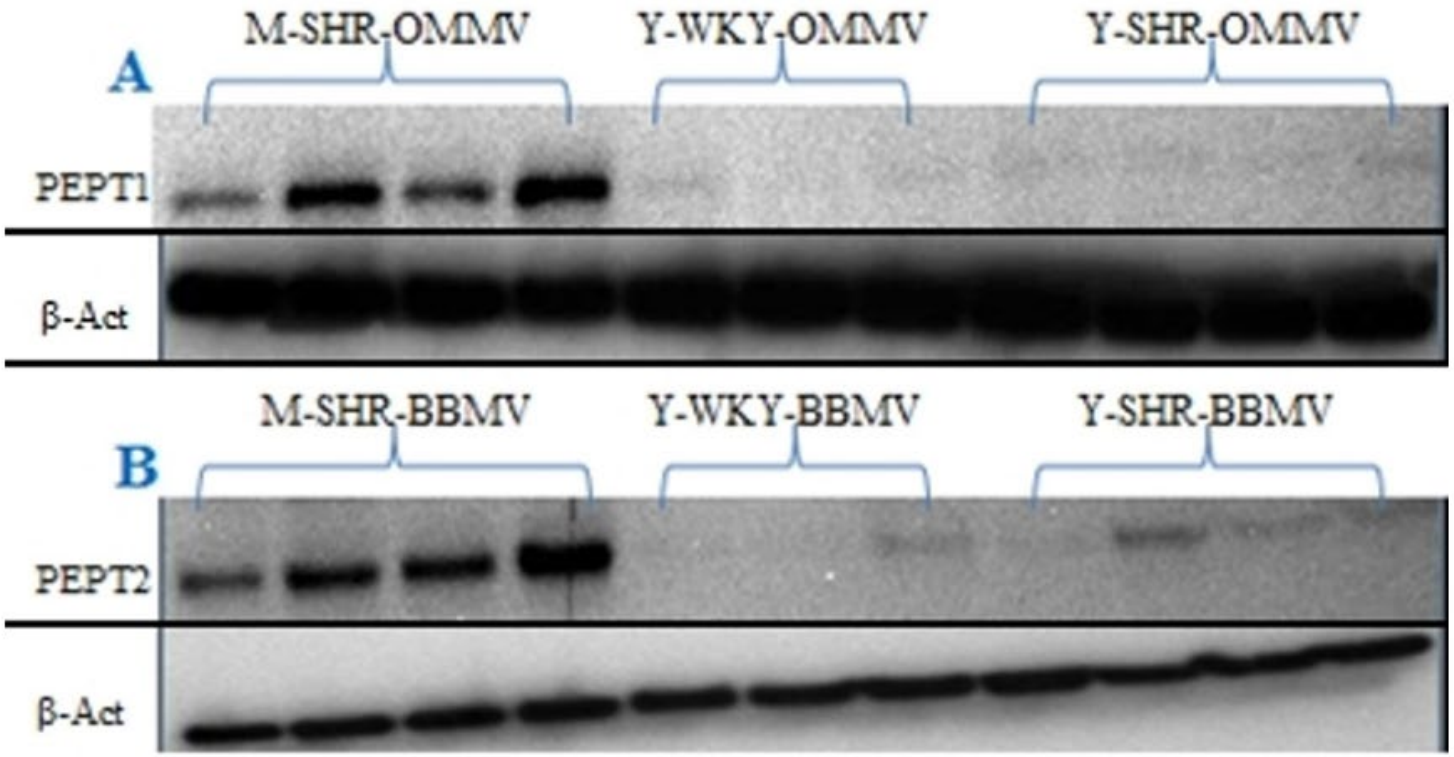
M-SHR-OMMV
Y-WKY-OMMV
Y-SHR-OMMV
A
PEPT1
β-Act
M-SHR-BBMV
Y-WKY-BBMV
Y-SHR-BBMV
B
PEPT2
β-Act

Figure 7

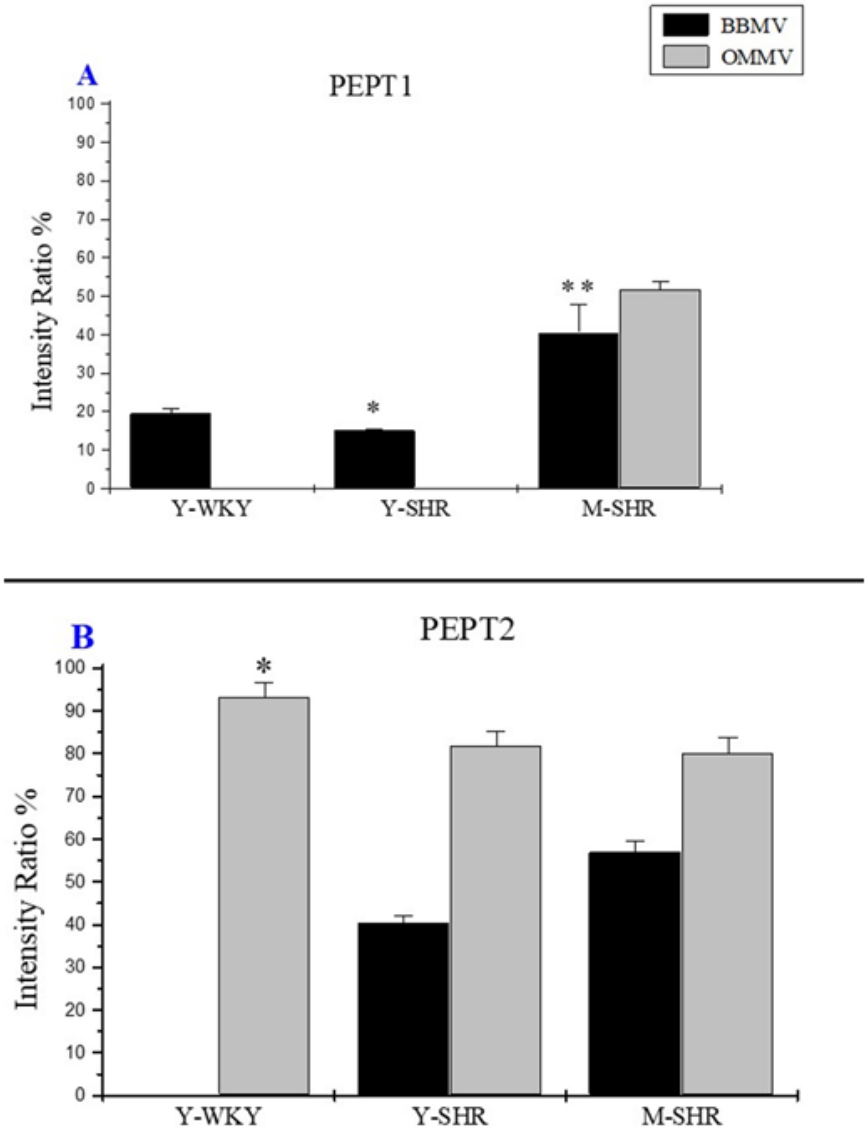
A
PEPT1
BBMV
OMMV
Intensity Ratio %
100
90
80
70
60
50
40
30
20
10
0
*
**
Y-WKY
Y-SHR
M-SHR
B
PEPT2
Intensity Ratio %
*
Y-WKY
Y-SHR
M-SHR

Figure 8

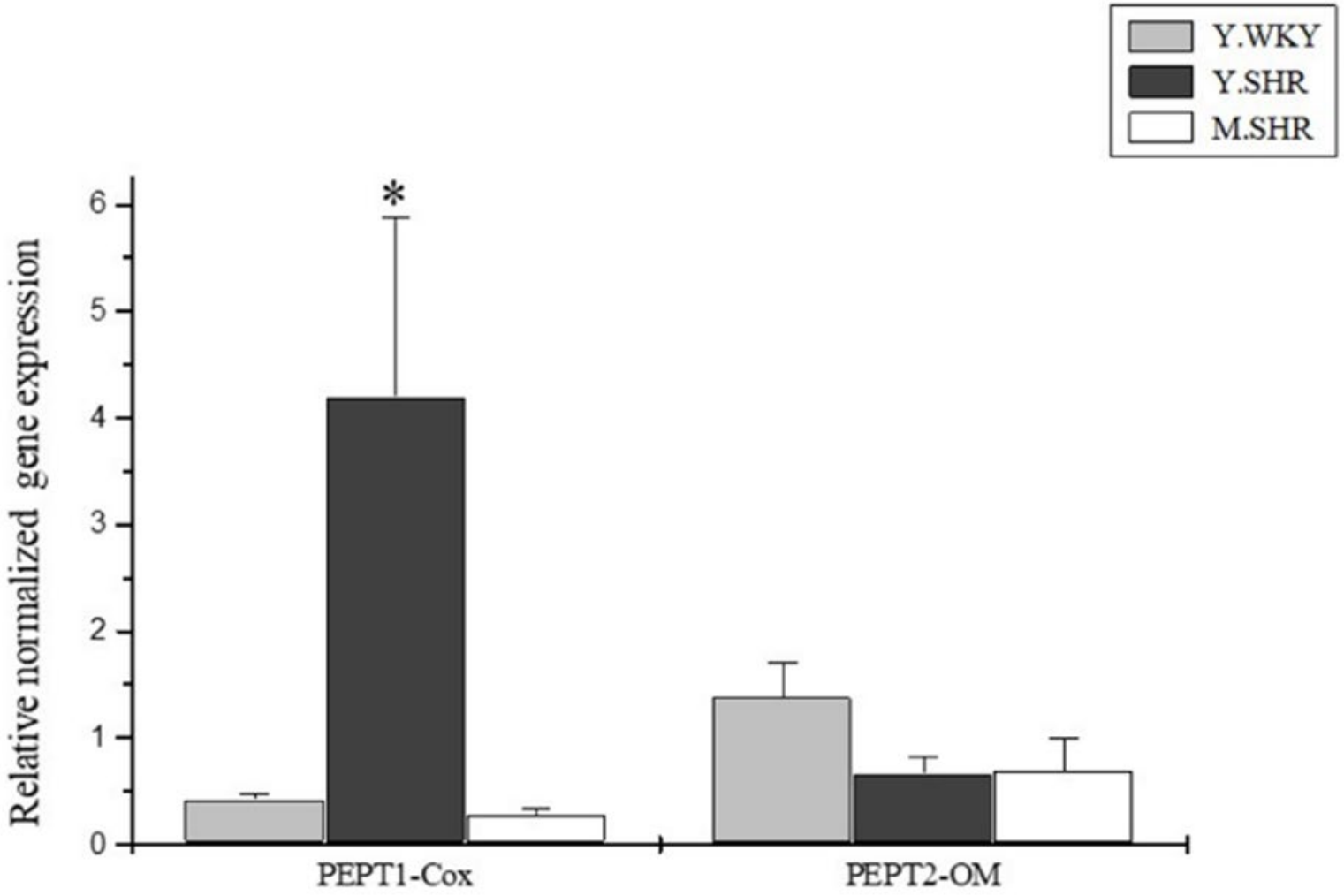
Y.WKY
Y.SHR
M.SHR
Relative normalized gene expression
0
1
2
3
4
5
6
*
PEPT1-Cox
PEPT2-OM